Evaluation of a Mixed Reality based Method
for Archaeological Excavation Support

Ronan Gaugne[1] , Théophane Nicolas[2], Quentin Petit [3], Mai Otsuki [4] and Valérie Gouranton[3]

[1]Univ Rennes, Inria, CNRS, IRISA, France
[2]Inrap, France
[3]Univ Rennes, INSA Rennes, Inria, CNRS, IRISA, France
[4]National Institute of Advanced Industrial Science and Technology (AIST), Tsukuba, Japan

Figure 1: *Left: Example of micro-excavation of a cremation urn. Right: the mixed reality environment designed in an archaeological context enables visualization inside a cremation urn.*

Abstract

In the context of archaeology, most of the time, micro-excavation for the study of furniture (metal, ceramics...) or archaeological context (incineration, bulk sampling) is performed without complete knowledge of the internal content, with the risk of damaging nested artefacts during the process. The use of medical imaging coupled with digital 3D technologies, has led to significant breakthroughs by allowing to refine the reading of complex artifacts. However, archaeologists may have difficulties in constructing a mental image in 3 dimensions from the axial and longitudinal sections obtained during medical imaging, and in the same way to visualize and manipulate a complex 3D object on screen, and an inability to simultaneously manipulate and analyze a 3D image, and a real object. Thereby, if digital technologies allow a 3D visualization (stereoscopic screen, VR headset ...), they are not without limiting the natural, intuitive and direct 3D perception of the archaeologist on the material or context being studied.

We therefore propose a visualization system based on optical see-through augmented reality that associates real visualization of archaeological material with data from medical imaging. This represents a relevant approach for composite or corroded objects or contexts associating several objects such as cremations. The results presented in the paper identify adequate visualization modalities to allow archaeologist to estimate, with an acceptable error, the position of an internal element in a particular archaeological material, an Iron-Age cremation block inside a urn.

CCS Concepts
● Human-centered computing → Virtual reality; ● Applied computing → Archaeology;

1. Introduction

The aim of the study presented in this manuscript is to propose a visualization system for archaeologists, and to evaluate its feasibility, its ergonomics, and the quality of visualization in 3D for analysis operations of incinerations. Such operations cover the identification of objects or bones, but also the measure of their density in the block and the observation of their fragmentation as well as their spatial relations. To do this, the questions of spatial perception are significant: the perception of depth, the location of data and object relations are relevant key elements. The user must have a good spatial perception in the sense of the sensory ability to collect maximum information on the positions of objects in the global space (size, distance, plans); as well as a good visualization which is the ability to identify the constituents of a local object (nature, measure, and shape). While the question of precision (in the metric sense) is inherent to these questions, it can not be the sole criterion of evaluation.

This problematic can be compared to medical concerns where some surgery operations require an accurate internal visualization to guide the surgeon. Augmented reality approaches are intensively investigated in this domain to improve surgery procedures [PNL*16, KBA*16, HKC*16] by displaying mixed renderings of real images and digital data on a 2D screen [CPB*14, HDP*13] or on a stereoscopic display [LISD10], or by adding visual clues directly on the patient's body either with projective AR [Hes10], [VPB*11] or with video see-through systems [SKBJR01, WSY*16].

2. Related work

X-ray vision that user can see the inside of the object is a popular research topic in Augmented Reality with specific challenges, as pointed out in [LDST13]. One of the popular methods is to create a virtual window (cutaway) on the real object surface and display only the inner object through this window [FAD02, SMK*09, SBMHN06] with video see-through systems. This method can improve observers' depth perception in AR. Livingston et al., in [LSG*03], utilized mobile AR in an urban environment and also conducted a user study to determine which drawing style and opacity settings best express occlusion relationships among far-field objects. Bichlmeier et al., [BWHN07], modified the real surface to be semi-transparent and then visualized the virtual object as though the observer viewed it through the semi-transparent area, using a video-see-through system. Another method that uses transparent surface with enhanced saliency information is presented in [KVZ*13].

In archaeology, approaches based on virtual reality, mixed reality or augmented reality are increasingly used in scientific processes. Virtual archaeology was first introduced by Reilly in 1990 and was initially presented for excavation recording and virtual re-excavation using multimedia technologies. In a similar way, Krasniewicz, [Kra00], proposed a 360 visualization infrastructure to help archaeologists in their research work. Augmented and mixed reality are widely used for cultural heritage valorization but remain seldom used for scientific purposes. On an archaeological site, during excavation operations, different types of archaeological material can be discovered, such as ceramics, metallic aggregates, and funeral material. Such material is difficult to analyze in-situ and is sent to a laboratory for extended analysis. Advanced image techniques such as MRI and CT scan provide internal viewing of the material that helps to identify the internal content and to optimize the preparation of the excavation, as pointed out in the works [SERPS10], and [NGT*18]. But this kind of image use remains still in a limited proportion due to the difficulties of carrying this type of analysis on a large scale with appropriate access to equipment and trained personnel, and for exploiting the obtained digital data. Furthermore, the mapping between the 2D data and the actual material requires a mental exercise for the practitioner that is not straightforward and can induce some mistakes in the evaluation of the internal spatial structure of the archaeological material.

In this paper, we compare different see-inside methods [OKM15, GOMC17] which overlays a virtual random-dot mask on the surface of a real object in a stereoscopic AR environment. Otsuki et al. [OKM15] have studied about the effectiveness of their method by comparing other typical methods (e.g. cut-away, semi-transparent) using simple and flat surfaces, with a video-see-through system. In particular, they observed that although semi-transparent mask also seemed to achieve a greater score than the cut-away and without mask conditions, there was no significant difference. Some participants of their experiments commented that semi-transparent mask did not markedly assist them in determining whether the circle was behind or in front of the mask. Ghasemi et al. [GOMC17] investigated the design principal of the mask, and surface information preservation using textured flat surfaces. We extend this method to more complex-shaped 3D objects and aims to evaluate the effectiveness under the particular situation assumed the practical usage; physical excavation of archaeological material.

3. Context of the work

3.1. Motivation of the work

Incinerated human remains can be grouped in urns of various materials or deposited directly in the ground. In recent years cinerary deposits have been perceived as a small-scale archaeological context as presented in [SMLG15], and [McK13]. This new status induced the implementation of protocols of search and registration with reasoned disassembly and segmentation in a series of passes. The result is a well-established protocol where, through methodical excavation in laboratory (see Figure 2), bones and any other artifacts are released, in order to identify and characterize components, to detect funeral gestures, and to restitute the external form of the deposit.

These excavation operations are accompanied by systematic graphical and photographical records to document the successive dismantling and spatialize the different artifacts. With this protocol, the visualization of the cluster in its entirety is impossible and the spatial visualization limited to the various successive slices and disassemblies. The anthropologist must therefore make a mental reconstruction work or have recourse to drawing to apprehend the cluster in its integrity, with a great difficulty to identify wall effects able to reveal the presence of a perishable content, or perishable items in the cluster. It also becomes very difficult to compare sev-

eral incinerations with each other. The excavation protocol of a funeral urn container is applied regardless of whether it is empty or the interesting part is grouped in a limited portion of the receptacle. These operations last several days for each block.

The block sampling of cinerary deposits for laboratory excavation enables the use of CT scan [PPMN15]. This process allows non-destructive access to the internal structure of objects, and immediacy of information such as nature, quantity, location of remains, or traces of biological activities. Upstream of the excavation, the imagery allows the implementation of a suitable protocol, and the planned organization of conservative measures [RCD*15, JPK*06]. Archaeologists emphasize the value of this tool, citing the saving of time, the predictability of the excavation, and the possibility of visual "feedback" during excavation.

Figure 2: *Micro-excavation of a cremation block in a funeral urn.* © *I. Le Goff (Inrap)*

3.2. Contribution of the work

Our work contributes with an optical see-through augmented reality framework, based on CT scan data, designed specifically to support archaeological study process. More precisely, we prefer to designate our framework as mixed reality as it combines at the same level a physical representation of archaeological material and a digital 3D representation of internal elements of this material. We present an evaluation of the efficiency of such system for archaeological studies. For this purpose, archaeologists were associated all along the project in order to design, and evaluate the mixed reality system.

Our work was performed in the context of a multidisciplinary collaboration between archaeologists and computer scientists started several years ago, with the aim to propose and design new tools and new practices for archaeologists, based on 3D technologies. The work was mainly driven by questions raised by archaeologists during the study of an Iron Age cremation urn.

3.3. Archaeological context

The archaeological material considered in this study comes from an Iron Age site housing ten cremation burials containing pottery vessels, excavated in 2014. The exceptional state of preservation of some of these cremations prompted archaeologists to use CT scan to analyze their contents. In some case, a number of metal objects were highlighted as in the F42A cremation (see Figure 3) containing a fibula and a knife blade. This particular urn, revealing an exceptional content has been completely dismantled to extract the artifacts. Its dimensions were 23x25x14 cm. These characteristics motivated the choice of this material for our study.
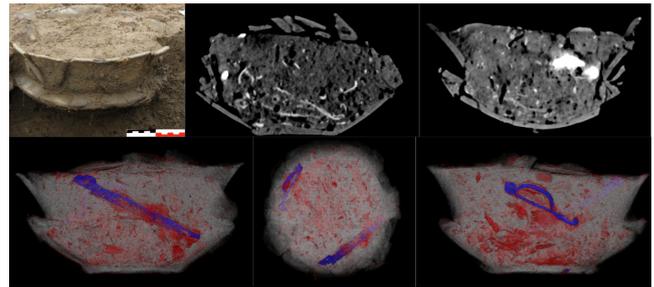
Figure 3: *Top Left: Cremation urn F42A. Top, middle and right: slice views from CT scan. Bottom: Volume rendering of the content of the F42A cremation.*

4. Method

The goal of the experiment is to explore how augmented reality can help a user for the spatial localization of an element inside archaeological material. The procedure designed for the experiment aims to reproduce a relevant situation of work with respect to the archaeological processes for the preparation of an excavation in laboratory.

4.1. Material

4.1.1. Digital data

The urn was digitized using a Siemens SOMATOM sensation 16 CT scan and the resulting data was used to produce two different 3D data, a 3D model of the urn and its content, and a physical 3D printed copy of the external surface of the urn. Technical parameters for the scan were 120 kV, 350 mAS, with a 512x512 matrix and a field of view of 320mm x 320 mm, resulting in a resolution of 625, and thickness of 1mm. We worked in an extended Hounsfield scale (from -10.000 to +40.000), to get a finer view of the metallic objects. The 3D model of the urn is composed of three meshes of different colors, generated using Osirix software , and post-processed using Blender and Meshlab. The first mesh, for the metallic parts, corresponds to the points whose radio-density is between 4500 and 10950, the second mesh, for the urn shape and sediments, between 700 and 1300, and the last mesh, for the bones parts, between 1600 and 2300. The 3D printing of the urn shape was printed on a Makerbot Replicator 2x, in two pieces, at 1:1 scale, with ivory ABS.

4.1.2. Apparatus

This experiment was conducted with a HoloLens, a mixed reality optical see-through headset to overlap the virtual 3D model to the 3D printing. The application was implemented with Unity 5.5.0f3 game engine using DirectX 11 rendering mode for x86 architecture. It was built for HoloLens with Visual Studio 15 Pro with UWP support on a Windows 10 computer. Performance wise, the demonstrator frame rate fluctuates from 20 to 30 fps with around 315k triangles displayed while looking at the urn on a 1268x720 px resolution.
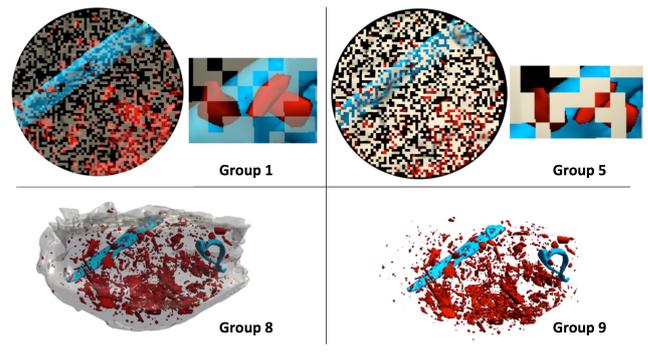
4.2. Visualization method

The optical see-through augmented reality system superimposes a rendering of the content of the funeral urn on a 3D printing of the external shape of the urn. We implemented different visualization metaphors, using virtual random-dot mask (RDM) [OKM15, GOMC17], and semi-transparent rendering, as the previous results on simpler contexts were promising. The RDM conveys to the observers the illusion of observing the inside through many small holes by showing the virtual objects in the non-dots area and showing the original surface in the dots area. While the number of elements inside the urn provides important depth cues, we think it is important to confirm whether the RDM remains effective in this case. Furthermore, because we have no knowledge whether the RDM is effective for 3D complex virtual object, we need to check various parameters. The variation of RDM methods is defined by a combination of 3 parameters which are dot density (25%, 50%), dot opacity (50%, 100%), and dot point size based on mask diameter (1/40 and 1/60 of the mask size). The texture of the dots area is the same as the texture of the surface of the urn. In order to validate the effectiveness of RDM method, we added a "no-dot" mask (NDM) display method, where the mask is rendered either completely transparent, either semi-transparent by alpha blending with an opacity of 50%. In both RDM and NDM, the objects inside the urn are displayed through a 10 cm diameter disk projected on the surface of the urn. The position of the mask is placed according to user's head orientation and centered on his viewpoint. Finally, in order to verify if the characteristics of shape and content of the urn were sufficient to carry enough depth cue for the user, we added a whole content display method where the content of the urn is rendered either directly, either through a semi-transparent rendering of the surface of the urn. We obtain a total of twelve different variations of the methods, each represented by a group Id starting with the value 0. The first eight groups correspond to the RDM groups characterized with their 3 parameters (dot opacity, dot density, dot size) as follow: $0(50, 50, 1/40)$, $1(50, 50, 1/60)$, $2(50, 25, 1/40)$, $3(50, 25, 1/60)$, $4(100, 50, 1/40)$, $5(100, 50, 1/60)$, $6(100, 25, 1/40)$, $7(100, 25, 1/60)$. The groups 8 and 9 correspond respectively to the with whole content display with semi-transparent surface and no surface. The groups 10 and 11 correspond respectively to the NDM group with transparent and semi-transparent masks. Some examples are shown in Figure 4.

The element to locate inside the urn is represented by a green sphere of diameter 5mm. This size corresponds to the average size of bones fragments. The color of the sphere was chosen to easily detect its position inside the urn. In order to define the possible positions of the target element, we considered a parallelepiped of 5.3x3x6.6 cm. The possible positions are defined as the eight vertices, the six centers of faces, the twelve centers of edges and the center of the parallelepiped, resulting in 27 possible positions (Figure 5).

4.3. Procedure

The procedure was designed in collaboration with an archaeologist to simulate a scenario where an anthropologist wants to see inside some material of study and try to locate one particular element. The global workflow of the experiment is organized in three phases, a

Figure 4: *Four different visualization modalities corresponding to variation 1, 5, 8 and 9.*
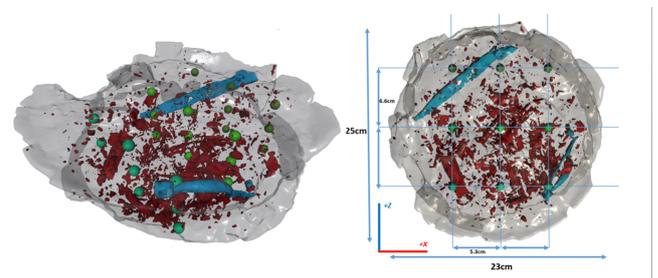
Figure 5: *All possible target positions.*

calibration phase, a tutorial phase and an experimental phase, presented thereafter.

The starting position of the participant, the relative position of the urn with respect to the participant, and the circular trajectory of the participant around the urn were the same in order to obtain comparable data (Figure 6).

Figure 6: *The participant performs one iteration of the experimentation and turns around the urn to localize the target. The starting and final position are materialized on the floor.*

Calibration phase: Before the experimentation, we adjusted the urn height based on the participant elbow height with a tripod support, so the angle while looking at the urn would stay in the same range of values (Figure 7, left). To match the position of the 3D model on the 3D printing, we used hand position recognized by

HoloLens and a basic GUI for small translation and scale offset. 3D printing urn rotation was similar for all participants.

Figure 7: *Left: Calibration of the urn height relative to the user's elbow. Right: Movement of the user during the experiment.*

Tutorial phase: 6 iterations of the experimentation with different visualization methods were proposed to the participants in order to familiarize them with the process.

Experimentation phase: The experimentation phase itself was a repetition of the same task with a variation of different parameters. The iterative task to be performed by the participant was divided in two steps. First, a localization step where the participant had to search for a target inside the 3D model of the urn and, second, an estimation step where the participant had to estimate the position of the target step. Participants started on a mark on the ground. They were asked to turn around the urn clockwise while looking for the target inside the urn through the current visualization method and then to come back at the mark to estimate the position of the target (Figure 6, Figure 7, right, and Figure 8, left). During the estimation of the position, all objects inside the urn were hidden including the target, and the surface was rendered semi transparently. The participant started by setting the depth of the vertical plane with their hand (figure 8, middle). Once the position of the plan was validated, the participant placed a point on this plane using headset orientation (figure 8, right). The participant used HoloLens clicker for all interactions, such as validation of an action or activation of a menu button. In the event of a manipulation error, it was possible to enter the input again.

Figure 8: *Left : Random dot-mask rendered on the 3D printed urn. Middle: cut plane moved with hand position. Right : Point on cut plane moved with head orientation.*

Iteration steps During the experimentation, we performed 6 repetitions per visualization method (6x12=72 iterations) with a constrained random position of the target among the 27 possible positions for each iteration. The constraint applied to the distribution of the targets was to have among the 6 iterations of a visualization method, 2 positions in the top 3x3 square, 2 positions in the middle 3x3 square, and 2 positions in the bottom 3x3 square. We

added this constraint because in our procedure, the user completely turn around the urn, so we expect the variations on X-axis (front to behind) and Z-axis (right to left) to be less significant than the variation on Y-axis (top to bottom). The overall sequence of iterations was randomly defined per participant. The dependent variable of the experiment was the error of the localization of the target defined as the distance between the center of the target sphere and the center of its estimated position.

4.4. Recorded data

As the experiment relies on a spatial perception of the user, we decided to evaluate the 3D perception of each participant with a short Vandenberg and Kuse mental rotation test composed of 12 questions to answer over a period of 3 minutes [VK78]. This test is based on 2D representations of rotations on 3D data. As archaeologists often work on 2D representations of their volume data, it is important to have a measure of the participants' spatial perception through 2D representation. We expect that archaeologists used to the gymnastic of this 2D/3D correlation should be comfortable with the spatial representation proposed in this work. At the end of the experiment, participants had to fill a questionnaire in order to gather subjective information about the level of localizability of the target considering each type of mask (7-Likert scale questionnaire). All participants data were recorded at the end of each iteration in two distinct files, one for processed data, like time spent, traveled distance, visualization method parameters and the position of the participant relative to the urn and the estimated target position, and another one for raw data like head position and rotation at any time during a iteration.

4.5. Hypotheses

According to the repetition of the target in the urn, we expect that the estimated position of the target is closer to its actual position than to the neighboring positions. So we expect an acceptable accuracy of less than 3 cm which is the minimal distance between two possible positions. We expect the RDM method to provide depth cues that help the user to estimate the position of the target within the urn. Archaeologists often have to correlate volume material and 2D representation. As the estimation of the position of the target is related to the ability of the user to spot the target within the volume of the urn, we expect that his/her spatial perception ability on a 2D representation will have an impact on the accuracy of the estimation.

Our hypotheses considering the design of the experiment were: [H1] Mean error is lower than 3cm for our use case. [H2] Lower error for random-dot mask (RDM) visualization methods. [H3] Lower error for people with a better spatial perception.

4.6. Participants

16 people participated in the experiment (4 Female, 12 Male), aged between 20 and 47 ($\bar{x} = 26.4; \sigma = 6.6$). Participants took on average 45 minutes to perform the experiment. All participants were informed about the procedure of the experiment and gave their informed consent without retribution.

5. Results

A Shapiro-Wilk test was performed to evaluate whether data follow a normal distribution. As the result showed significant at the 5% level we analyzed the results with a Friedman non-parametric test and post-hoc Wilcoxon signed-rank tests was conducted with a Bonferroni correction applied. The dependent variables analyzed were the distance between the estimated position and the actual position of the target (error), the time to locate the target, the position of the target on xyz axes and the result of the questionnaires.

5.1. Effect of the visualization method on error

There was a statistically significant difference in error depending on which visualization method was used $\chi^2(11) = 26.38, p = 0.0057$. Post-hoc analysis was conducted with a Bonferroni correction applied, resulting in a significance level set at $p < 0.00076$. There were no significant differences in all 66 pairs tested. Thus we cannot conclude that visualization methods significantly impact the error even if there is a difference between some groups. The results are presented in Figure 9.
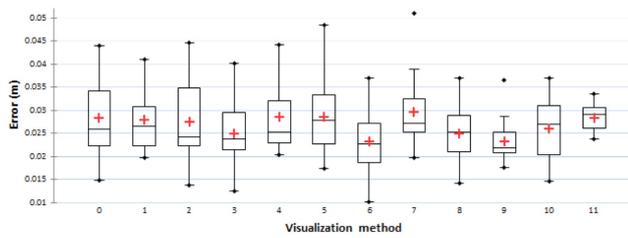

Figure 9: *Error for each visualization method.*

5.2. Effect of target axes on error

As we collected positions of the target on all the axis thanks to the repartition of the positions, we can look for effect on each axis independently. There was no statistically significant difference in the error depending target X offset $\chi^2(2) = 3.88, p = 0.14$ and target Z offset $2(2) = 4.88, p = 0.087$. Post-hoc analysis was conducted with a Bonferroni correction applied, resulting in a significance level set at $p < 0.017$. Medians (IQR) error for the target negative (lower layer), null (middle layer) and positive (higher layer) Y offsets were 3.1 (2.6 to 4.2), 2.6 (2.20 to 2.8) and 2.29 (1.9 to 2.6) cm, respectively. There was no significant difference between the positive and the null offsets ($Z = -1.913, p = 0.056$). However there were a statistically significant difference in the negative Y offset against the positive Y offset ($Z = -3.154, p = 0,0016$) and in the negative Y offset against the null Y offset ($Z = -3.156, p = 0,0004$). The results are presented in Figure 10.

5.2.1. Effect of spatial perception on error

The Vandenberg and Kuse mental rotation test score [VK78] was used as a spatial perception performance indicator. A significant regression equation between the spatial perception and the error of the localization, presented in figure 11, was found ($F(1,13) =$
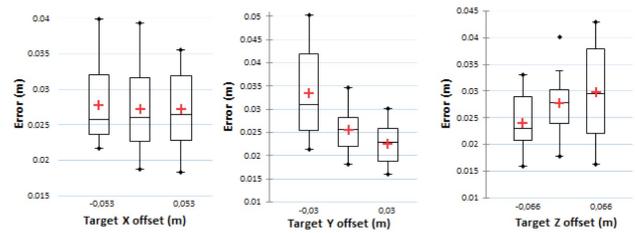

Figure 10: *Error for each axis target offset.*

$10.189, p = 0.007$), with a R^2 of 0.439: Participants' predicted error is equal to $3.6 - 0.2(PS)cm$ when PS is the perception score (number of points in the Vandenberg and Kuse test).
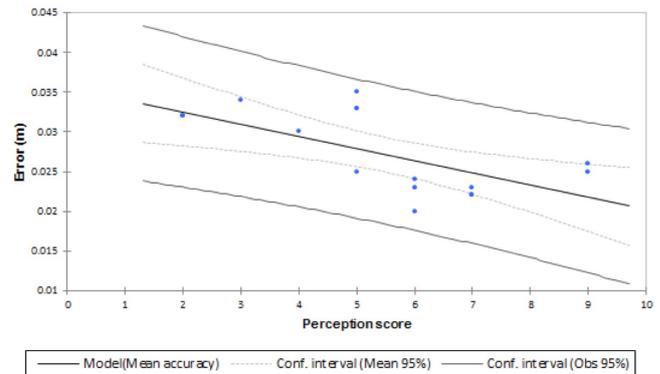

Figure 11: *Regression of mean error by perception score.*

5.3. Questionnaires

Participants were asked to evaluate for each method how convenient was the method to find the target, to estimate the position of the target and to perform the task in general. The rating used a 7-Likert scale where 1 meant the method described was bad and 7 meant that the method described was good for the given question. As illustrated in figure 12, participants widely preferred visualization method without mask (Group 8-11). They did not find RDM methods (Group 0-7) convenient, especially with high density and opacity values which get negatives feedback mostly because it was harder to see inside the object with these methods.

6. Discussion

We measured a mean error value of 2.67cm ($\sigma = 1.53cm$), which match our expectation to locate the small target, and validate the hypothesis [H1]. The procedure allows to locate the position of the target with an acceptable error with respect to the usage. In our usage case, RDM visualization method do not improve error or speed compared to other visualization methods, invalidating hypothesis [H2]. Our data show that the different visualization methods based on random-dot masks do not impact error. This can be explained by a major difference in the protocol of the experiment where participants could turn around the urn, with respect to the protocol used
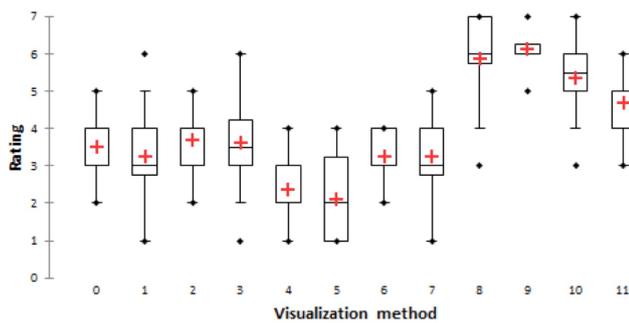
Figure 12: *Rating for each visualisation method.*

in [OKM15] where they remained seated. Therefore, in our experiment, participants could use the motion parallax cues and perceived the depth more easily than the case of the previous experiment. Furthermore, the different bones fragments and objects present inside the urn, and the irregular shape of the urn, gave many cues on the spatial localization of the target. The regression equation brought out between error and spatial perception shows that participant spatial perception has a positive impact on the error and thus validates the hypothesis [H3].

Due to lack of space we presented the most significant results with respect to the focus of the experiment. We also measured the time of each iteration, which revealed a better efficiency for groups 8 and 9 that provide a better overall view of the urn and its content.

We were able to notice some drawbacks of the apparatus used during the experiment. Even with ground markings, participants didn't reposition themselves on the same exact spot each time, mostly because their attention was too focused on the urn looking for the target. The holograms virtual model displayed by the HoloLens tends to drift (up to 2cm) while moving due to limitations in the tracking of the HoloLens. We were asking participants to reposition 3D printed urn to fit the 3D model one when an offset appeared during a pause moment between two iterations. In order to improve the usability of the method, the system has to integrate automated calibration and tracking with respect to the real object. The HoloLens tracking system could handle this feature, but at the cost of a loss of performance. A better solution would be to integrate an additional external optical tracking system that communicates with the HoloLens.

The optimal zone to display holograms with the HoloLens is between 1.25 and 5 meters. However, due to the nature of the experiment, participants were most of the time closer than these values and were on average at 56,6 cm from the urn ($\sigma = 6,9cm$). It is also recommended to aim for 60 fps to minimize latency and improve participant experience, but our framerate application remained capped at 30 fps despite many optimizations. Those limitations may have magnified visual artefacts reported by some participants like dot flickering with random-dot mask methods.

From the "archaeologist" user's point of view the test is particularly conclusive. The AR system is perfectly adapted to the case of use: to see what is invisible because hidden inside another object (here bones and metal furniture inside a funerary urn). The use,

past the phase of handling the material, is very intuitive and allows to analyze a cinerary urn, with the possibility of associating other related tasks such as taking notes, but also to share the user's visualization to third parties via the video feedback of the user's point of view. If in use the system is intuitive, it nevertheless has some defects inherent in the apparatus that were noticeable during the test such as the care of the interface, or the weight of glasses during extended use, which only have an impact at the margin compared to the interest of this type of visualization. While the arbitrary texture associated with the meshes cannot allow to determine the nature of the objects, the relevance of the visualization of their shape and scale is most often sufficient to express important preliminary observations.

The gain of a 3D visualization of the interior of an incineration before any manual intervention via the cuts or the reconstructions by the tomodensitometry is already of a great interest. In the case of incineration in a container, the first information delivered by the CT scan of cinerary deposits is the state of conservation of the urn: it is possible to see the internal deformations of the vessel (sedimentary pressure), the fragmentations and cracking and to measure the impact on the integrity of the deposit itself.

The radiographic procedure makes it possible to immediately understand the level of bone filling in the urn, its appearance on the surface and to identify, in a very precise manner, bioturbations (roots, biological activities of earthworms, etc.). But the possibility of associating the real (cinerary urn) and 3D models from reconstruction is perceived by the archaeologist user as a revolution. In addition to the experimentation, the system was presented to archaeologists expert in the study of such material. They confirmed the good spatial perception and were able to precisely identify 8 different plans of depth, i.e. to differentiate up to 8 elements one behind the other, within the urn, to correctly locate the different artefacts and evaluate the distance between them.

The experimentation was meant to evaluate the estimation of the position of some element inside the archaeological material. Further investigations are required to evaluate the efficiency of the system in an actual micro-excavation process, with an emphasis on the analysis of the internal content, and of the spatial organization of the elements.

7. Conclusions

The experiment presented in this paper explored different modalities of visualization of the internal structure of archaeological material, based on mixed reality, in order to evaluate their efficiency in the context of a work process such as a micro-excavation. The mixed reality based method allowed to superimpose 3D models of the interior of the material, obtained by CT scan, on a 1:1 copy of the real urn, and offered the archaeologist a vision in transparency of the object.

The different modalities of visualization proposed to the participants did not differ significantly in term of performance. However, in term of comfort and efficiency, the participants preferred the modalities offering the most complete visualization of inside the urn.

The resulting visualization method appears to be accurate

enough to envisage the possibility of carrying out technical excavation procedures (removing sediment, bones or other) on a "real" cinerary urn. It allows an analysis in 3D, and can also guide archaeologists in search and excavation operations through virtual enhancement. Nevertheless, further works are required to use the system in accompaniment of an actual excavation. A video of this work is available at https://vimeo.com/349677053.

Acknowledgements

References

[BWHN07] BICHLMEIER C., WIMMER F., HEINING S. M., NAVAB N.: Contextual anatomic mimesis hybrid in-situ visualization method for improving multi-sensory depth perception in medical augmented reality. In *6th IEEE and ACM Int. Symp. on Mixed and Augmented Reality (ISMAR)* (2007), pp. 129–138. 2

[CPB*14] COLLINS T., PIZARRO D., BARTOLI A., CANIS M., BOURDEL N.: Computer-assisted laparoscopic myomectomy by augmenting the uterus with pre-operative mri data. In *IEEE Int. Symp. on Mixed and Augmented Reality (ISMAR)* (2014), pp. 243–248. 2

[FAD02] FURMANSKI C., AZUMA R., DAILY M.: Augmented-reality visualizations guided by cognition: Perceptual heuristics for combining visible and obscured information. In *IEEE Int. Symp. on Mixed and Augmented Reality (ISMAR)* (2002), pp. 215–320. 2

[GOMC17] GHASEMI S., OTSUKI M., MILGRAM P., CHELLALI R.: Use of random dot patterns in achieving x-ray vision for near-field applications of stereoscopic video-based augmented reality displays. *PRESENCE: Teleoperators and Virtual Environments 26*, 1 (2017). 2, 4

[HDP*13] HAOUCHINE N., DEQUIDT J., PETERLIK I., KERRIEN E., BERGER M.-O., COTIN S.: Image-guided simulation of heterogeneous tissue deformation for augmented reality during hepatic surgery. In *IEEE Int. Symp. on Mixed and Augmented Reality (ISMAR)* (2013). 2

[Hes10] HESS H. A.: A biomedical device to improve pediatric vascular access success. *Pediatr Nurs 36*, 5 (2010), 259–263. 2

[HKC*16] HAMACHER A., KIM S. J., CHO S. T., PARDESHI S., LEE S. H., EUN S.-J., WHANGBO T. K.: Application of virtual, augmented, and mixed reality to urology. *International neurourology journal 20*, 3 (2016), 172. 2

[JPK*06] JANSEN R. J., POULUS M., KOTTMAN J., DE GROOT T., HUISMAN D. J., STOKER J.: Ct: a new nondestructive method for visualizing and characterizing ancient roman glass fragments in situ in blocks of soil. *Radiographics 26*, 6 (2006), 1837–1844. 3

[KBA*16] KHOR W. S., BAKER B., AMIN K., CHAN A., PATEL K., WONG J.: Augmented and virtual reality in surgery—the digital surgical environment: applications, limitations and legal pitfalls. *Annals of translational medicine 4*, 23 (2016). 2

[Kra00] KRASNIEWICZ L.: Immersive imaging technologies for archaeological research. *BAR INTERNATIONAL SERIES* (2000). 2

[KVZ*13] KALKOFEN D., VEAS E., ZOLLMANN S., STEINBERGER M., SCHMALSTIEG D.: Adaptive ghosted views for augmented reality. In *2013 IEEE Int. Symp. on Mixed and Augmented Reality (ISMAR)* (2013), pp. 1–9. 2

[LDST13] LIVINGSTON M. A., DEY A., SANDOR C., THOMAS B. H.: Pursuit of x-ray vision for augmented reality. In *In Human Factors in Augmented Reality Environments*, Tony Huang L. A., Livingston M., (Eds.). Springer, USA, 2013, pp. 67–107. 2

[LISD10] LIAO H., INOMATA T., SAKUMA I., DOHI T.: 3-d augmented reality for mri-guided surgery using integral videography autostereoscopic image overlay. *IEEE Transactions on Biomedical Engineering 57*, 6 (June 2010), 1476–1486. 2

[LSG*03] LIVINGSTON M. A., SWAN J. E., GABBARD J. L., HOLLERER T. H., HIX D., JULIER S. J., BAILLOT Y., BROWN D.: Resolving multiple occluded layers in augmented reality. In *2nd IEEE and ACM Int. Symp. on Mixed and Augmented Reality (ISAMR)* (2003). 2

[McK13] MCKINLEY J. I.: Cremation: Excavation, analysis, and interpretation of material from cremation-related contexts. In *In The Oxford Handbook of the Archaeology of Death and Burial*, Stutz L. N., Tarlow S., (Eds.). Oxford University Press, UK, 2013. 2

[NGT*18] NICOLAS T., GAUGNE R., TAVERNIER C., MILLET E., BERNADET R., GOURANTON V.: Lift the veil of the block samples from the Warcq chariot burial with 3D digital technologies. In *Digital Heritage 2018 - 3rd International Congress & Expo, IEEE* (San Francisco, United States, 2018), pp. 1–8. 2

[OKM15] OTSUKI M., KUZUOKA H., MILGRAM P.: Analysis of depth perception with virtual mask in stereoscopic AR. In *Int. Conf. on Artificial Reality and Telexistence and Eurographics Symposium on Virtual Environments, ICAT-EGVE, Kyoto, Japan, Oct. 2015.* (2015). 2, 4, 7

[PNL*16] PELARGOS P., NAGASAWA D., LAGMAN C., TENN S., DEMOS J., J. LEE S., BUI T., E. BARNETTE N., BHATT N., UNG N., BARI A., MARTIN N., YANG I.: Utilizing virtual and augmented reality for educational and clinical enhancements in neurosurgery. *Journal of Clinical Neuroscience 35* (10 2016). 2

[PPMN15] PANKOWSKA A., PRUCHOVA E., MONIK M., NOVAKOVA M.: Taphonomy of cremation burials: excavation and deposition bias in bone preservation. *Archäologische Arbeitsgemeinschaft Ostbayern/West- und Südböhmen/Oberösterreich* (06 2015), 223–233. 3

[RCD*15] RE A., CORSI J., DEMMELBAUER M., MARTINI M., MILA G., RICCI C.: X-ray tomography of a soil block: A useful tool for the restoration of archaeological finds. *Heritage Science 3*, 4 (01 2015). 3

[SBMHN06] SIELHORST T., BICHLMEIER C., MICHAEL HEINING S., NAVAB N.: Depth perception – a major issue in medical ar: Evaluation study by twenty surgeons. vol. 9, pp. 364–72. 2

[SERPS10] STELZNER J., EBINGER-RIST N., PEEK C., SCHILLINGER B.: The application of 3d computed tomography with x-rays and neutrons to visualize archaeological objects in blocks of soil. *Studies in Conservation 55* (06 2010), 95–106. 2

[SKBJR01] SAUER F., KHAMENE A., BASCLE B., J. RUBINO G.: A head-mounted display system for augmented reality image guidance: Towards clinical evaluation for mri-guided neurosurgery. In *4th Int. Conf. on Medical Image Computing and Computer-Assisted Intervention (MICCAI)* (London, UK, 10 2001), vol. 2208, Springer-Verlag. 2

[SMK*09] SCHALL G., MENDEZ E., KRUIJFF E., VEAS E., JUNGHANNS S., REITINGER B., SCHMALSTIEG D.: Handheld augmented reality for underground infrastructure visualization. *Personal Ubiquitous Comput. 13*, 4 (May 2009), 281–291. 2

[SMLG15] SANSON L., MAESTRACCI J., LE GOFF I.: De la méthode d'enregistrement de terrain à l'analyse spatiale des structures funéraires. l'exemple des structures funéraires de remilly-les-pothées (ardennes). 2

[VK78] VANDENBERG S. G., KUSE A. R.: Mental rotations: A group test of three-dimensional spatial visualization. *Perceptual and motor skills 47* (11 1978), 599–604. 5, 6

[VPB*11] VOLONTE F. G. D., PUGIN F. L., BUCHER P. A. R., SUGIMOTO M., RATIB O., MOREL P.: Augmented reality and image overlay navigation with osirix in laparoscopic and robotic surgery: not only a matter of fashion. *Journal of Hepato-Biliary-Pancreatic Sciences 18*, 4 (2011), 506–509. 2

[WSY*16] WANG J., SUENAGA H., YANG L., KOBAYASHI E., SAKUMA I.: Video see-through augmented reality for oral and maxillofacial surgery. *Int. Journal of Medical Robotics and Computer Assisted Surgery 13* (06 2016). 2